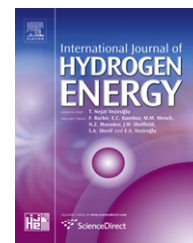


Available at [www.sciencedirect.com](http://www.sciencedirect.com)journal homepage: [www.elsevier.com/locate/he](http://www.elsevier.com/locate/he)

# Non intrusive diagnosis of polymer electrolyte fuel cells by wavelet packet transform

Nadia Yousfi Steiner<sup>a,\*</sup>, Daniel Hissel<sup>b</sup>, Philippe Moçotéguy<sup>a</sup>, Denis Candusso<sup>c</sup>

<sup>a</sup> EIFER, European Institute for Energy Research, Emmy-Noether Str., 11, Karlsruhe, Germany

<sup>b</sup> FEMTO-ST/ENISYS/FCLAB, UMR CNRS 6174, University of Franche-Comté, rue Mieg, 90010 Belfort Cedex, France

<sup>c</sup> INRETS/FCLAB, The French National Institute for Transport and Safety Research, rue Mieg, 90010 Belfort Cedex, France

## ARTICLE INFO

### Article history:

Received 29 July 2010

Received in revised form

8 October 2010

Accepted 11 October 2010

Available online 18 November 2010

### Keywords:

Polymer electrolyte fuel cell (PEFC)

Diagnosis

Flooding

Drying out

Degradation

Wavelet packet transform

## ABSTRACT

Fuel cell is a promising technology for both automotive and stationary applications. However, its reliability and its lifetime remain major hurdles to its wide access to these markets.

It is therefore necessary to develop reliable diagnosis tools adapted to these two applications' requirements. More particularly, online and real time tools for diagnosis will permit an early faults diagnosis and therefore an increase of the system reliability and performance.

Most of the existing fault diagnosis methodologies in fuel cells require the knowledge of numerous parameters that may lead to a special inner parameter monitoring setup, which is difficult, even impossible to obtain, considering constraints like fuel cell stacks' geometry. Moreover, considering the final fuel cell stack end-uses, for instance in transportation applications in which the "on-board" instrumentation has to be minimized, a model using a minimal number of parameter is highly desirable.

In this paper, a simple and low-cost flooding diagnosis method applied to a PEFC (Polymer Electrolyte Fuel Cell) is described. This method only uses the stack voltage and can be adapted to a large set of fuel cell configurations and applications.

Coming from the signal-processing domain, the diagnosis consists in a signal feature extraction by multiscale decomposition using discrete wavelet transform, followed by fault identification and classification. Results obtained in this work showed that the wavelet analysis method allows the identification of the flooding based on the patterns obtained from the wavelet packet coefficients.

The application of wavelet theory to fuel cell diagnosis is innovative and very promising and the experimental results obtained in this study proved its feasibility and reliability to classify correctly PEFC experimental states into flooded and non-flooded state of health.

© 2010 Professor T. Nejat Veziroglu. Published by Elsevier Ltd. All rights reserved.

## 1. Introduction

Because of its low CO<sub>2</sub> emissions, its high power density and efficiency, the Polymer Electrolyte Fuel Cell (PEFC) technology appears as a promising alternative to the existing power converters. However, to be fully adapted to transportation and

stationary applications, the reliability and lifetime are important barriers to be overcome. In a PEFC stack, many critical operations can cause power decay or even failure, reducing the system reliability and shortening its lifetime. Water management, for instance, is still a major cause of power decay [1,2]. In fact, while PEFC operation is fundamentally linked to the

\* Corresponding author. Tel.: +49 72161051338; fax: +49 72161051332.

E-mail addresses: [nadia.steiner@eifer.uni-karlsruhe.de](mailto:nadia.steiner@eifer.uni-karlsruhe.de) (N.Y. Steiner), [daniel.hissel@univ-fcomte.fr](mailto:daniel.hissel@univ-fcomte.fr) (D. Hissel), [philippe.mocoteguy@eifer.uni-karlsruhe.de](mailto:philippe.mocoteguy@eifer.uni-karlsruhe.de) (P. Moçotéguy), [denis.candusso@inrets.fr](mailto:denis.candusso@inrets.fr) (D. Candusso).

0360-3199/\$ – see front matter © 2010 Professor T. Nejat Veziroglu. Published by Elsevier Ltd. All rights reserved.

doi:10.1016/j.ijhydene.2010.10.033

presence of water molecules, an optimal equilibrium between introduced, exiting and produced water inside the cell is hard to set. On the one hand, water permits proton conduction in the ionomeric phase of both membrane and catalyst layer, and drying might cause a rapid rise of ohmic losses and leads, in case of long exposure, to membrane mechanical degradation. On the other hand, water accumulation in the electrode may induce a cell “flooding” impeding the gases from reaching the catalyst layer, which causes redoubtable fuel/oxidant starvation problems [3,4]. Therefore, a reliable diagnosis and supervision technology of a fuel cell stack during operation is highly desirable.

Studies investigating the reliability of the PEFCs have been conducted in the last few years [1,3–6], trying to understand the degradation mechanisms and to improve fuel cell reliability. Modeling is a common way to reach that aim [7]. However, physical modeling needs the knowledge of many parameters that are not always easy to monitor in complex systems such as fuel cell generators. Furthermore, the transportation application requirement that aims at minimizing the embedded devices allows only a minimal instrumentation.

To overcome this problem, works involving non intrusive diagnosis methods and analyzing only the cell response to given solicitations in case of faulty operation have been developed. In such studies, the fuel cell acts as “self-sensor” which is of great help, considering the problems drawn above. Tian et al. [8], for example, developed a methodology based on the analysis of the Open Circuit Voltage (OCV) responses to pressure solicitations in order to detect the cells that show abnormal performance and voltage patterns. This work leads to a simple detection tool, since it uses only stack’s OCV response as a diagnosis parameter. In another work, Hissel et al. [9] developed a simple fuzzy diagnosis model tuned using “genetic algorithms” in order to detect two types of faults, namely membrane drying and water and/or nitrogen accumulation. Both degradation states were efficiently separated.

Coming from the signal-processing domain, the Fourier Transform (FT) is one of the most widely known methods used for fault diagnosis. Chen and Zhou [10] used this method to correlate the stack voltage evolution with the pressure drop signal across the electrodes. The dominant frequency of cathode pressure drop was analyzed to predict the sudden stack voltage evolution indicating a flooding. Unfortunately, even if the FT-based methods lead to fine frequency resolution, they are not adapted to non-stationary signals, which are typically those extracted from the fuel cell during operation.

Due to their time-frequency localisation properties, wavelet and wavelet packet transform seem to be appropriate for feature extraction and classification. They allow the extraction of rich information compared to diagnosis methods based on time features only.

Based on this method, several diagnosis approaches have been developed, including time-scale analysis of the signals as well as features extraction for fault detection and identification. This latter application can be considered as a typical “pattern recognition” (PR) problem, where the important information contained in the signals is showed up, allowing the use of the relevant features in fault diagnosis. Diagnosis based on wavelet has been used in many application fields

such as machine condition monitoring [11,12], medicine where good results has been published about diagnosis by analyzing the hearth sound signals [13] or by feeding brain computer interfaces [14] as well as identifying pathologies from speech signal analysis [15].

In the chemical applications, some works presented a diagnosis based on wavelets, for instance to analyze signals coming from the gases sensors in order to discriminate different Chinese vinegars [16]. The common point between these works is the extraction of the relevant information from the studied signal (or image) using wavelets transform in order to characterize and discriminate different faults.

In this work, we propose to use wavelets in order to discriminate between “flooding” and “non flooding” states of health in a PEFC. The wavelet decomposition is applied to stack voltage signals, recorded in these two different states of health. This method relies entirely on the measured data without considering the system structure.

The developed diagnosis method is simple, low-cost and minimal stack monitoring. It could be adaptable to a large set and size of fuel cells and to different applications (stationary, portable and transportation). Moreover, its use in fuel cell domain is innovative, and experimental results show good potentials in fuel cells diagnosis domain.

## 2. Diagnosis principle

In the last 20 years, the wavelets have experienced a growing interest [17–19]. They are today a link between mathematicians and engineers having a big success in signal-processing domain. The Wavelet Transform (WT) belongs to the multi-resolution analysis methods class: it permits examination of the signal and its local features under different scale and time localizations, which seems to be adapted to the fuel cell voltage signals.

The method developed in this study needs only the stack voltage as information to distinguish between a “flooding” and a “non flooding” state of health, because it is a rich “collection” of information about all the phenomena that lead to a given state of health. These phenomena could be distinguishable at different scales, using a “mathematical microscope” like the WT analysis. Moreover, the individual cell voltages can also be considered since flooding can occur only in a limited number of cells without significantly affecting the whole stack voltage.

In this work, as shown in Fig. 1, a signal (stack voltage) is treated by WT analysis to extract a “feature vector”, corresponding to a set of parameters that describes the signal using a multiscale decomposition. These features are finally used in order to discriminate between two states of health, namely “flooding” and “non flooding”.

### 2.1. Feature extraction and signal classification

#### 2.1.1. Discrete wavelet and wavelet packet decomposition

Wavelets are families of basis functions satisfying a certain number of mathematical criteria that transform the time

domain into a time-scale plane. In fact, wavelets family (which play the role of the analyzing function in the FT) are obtained by translation and dilations of a “mother” function  $\psi$ . Wavelet transform analysis uses localized waveforms (wavelets) in order to transform the analyzed signal into another representation helping to highlight certain information of interest. On a mathematical point of view, the WT is a convolution of a signal  $S$  with the wavelet function. The transformed signal obtained by continuous wavelet decomposition is expressed by [19]:

$$C_s(a, b) = \frac{1}{\sqrt{a}} \int_{-\infty}^{+\infty} s(t) \psi \left( \frac{t-b}{a} \right) dt \quad (1)$$

where  $S(t)$  is the signal to be analyzed,  $a$  the dilatation or the scale parameter,  $b$  the time translation parameter, the asterisk indicates the complex conjugate and the “wavelet coefficients” or “detail coefficients”  $C_s(a, b)$  represent the “similarity” between the signal and the basis wavelet function at each time and scale. The higher these coefficients are, the more similar the wavelet and the signal are. Fig. 2 illustrates this procedure for given signal  $S(t)$  at respective scale and translation parameters  $(a_1, b_1)$  and  $(a_2, b_2)$ .

For each scale parameter, the translation parameter describes the x-axis. This leads to different wavelets and the correlation between these wavelets and the signal are calculated: it corresponds to a set of wavelet coefficients. The bigger the wavelet coefficient is, the more similar are the wavelet and the signal patterns.

In case of “logarithmic dyadic discretization” [17] of  $a$  and  $b$  ( $a = 2^j$  and  $b = k \cdot 2^j$ ,  $j, k \in \mathbb{Z}$ ), Eq. (1) becomes: with  $j, k \in \mathbb{Z}$

$$C_s(j, k) = C_{j,k} = \frac{1}{\sqrt{2^j}} \int s(t) \psi \left( \frac{t - k2^j}{2^j} \right) dt \quad (2)$$

where  $j$  represents the scale variations and  $k$  the time translation variation.

In this specific case, the wavelet decomposition algorithm is equivalent to filtering the signal successively using a low-pass and a high-pass filter [17]. At the first decomposition level, the signal is decomposed into Approximation  $A$  (i.e., the low-pass filter output) and Detail  $D$  (i.e. the high-pass filter output). At the following levels, only the approximation signals will be filtered in the same way (Fig. 3(a)).

Since the WT decomposes only signal approximations, some problems may be encountered in applications where the important information is located in higher frequency domain. To overcome this problem, one can use Wavelet Packet decomposition, which is more “complete”. It consists in decomposing the approximation signal and also the detail signal, resulting then in richer information [19] (Fig. 3(b)). In Fig. 3(a) and (b), the signal  $S$  is decomposed at level  $j = 3$  (“A” corresponds to Approximation signal and “D” to detail. AD for instance means “Approximation of the detail”).

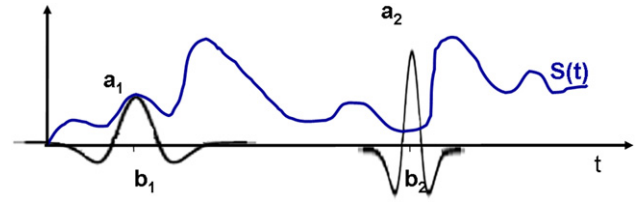


Fig. 2 – Illustration of the wavelet decomposition.

Therefore, with the WP decomposition, no information is lost: it is contained in a WP tree and remains available for use. WP transform is often described as a generalization of the discrete wavelet transform.

The analyzed signal is thus completely represented by a collection of “wavelet packets”. In a WP decomposition, a packet corresponds to a decomposition’s branch point or end-level. In case of Fig. 3b example, 14 packets can be identified: the two signals generated by first level decomposition, the 4 signals generated by second level decomposition and the 8 signals generated by third level decomposition. WP decomposition is thus, a good candidate for characteristics detection and allows reliable classification.

Finally, after a full decomposition of the signal, the normalized energy contained in a specific wavelet packet  $p$  is given by

$$E^p = \frac{1}{N_p} \sum_{j,k} |C_{j,k}^p|^2, \quad p = 1, \dots, 14 \quad (3)$$

where  $p$  indicates the packet number (defined in top down direction and, for a given line, in left right direction),  $C_{j,k}^p$  are therefore the coefficients contained in the packet  $N^\circ p$  and  $N_p$  the number of coefficients in the packet  $p$ .

This value is calculated for each packet. In the following sections, we will compare the energy contained in each packet of the WP transform.

### 2.1.2. Feature definition

For each wavelet packet, a certain number of parameters can be calculated from coefficients (their average value, their standard deviation, their total energy,...) so as to characterize a specific fault class (“flooding” and “no flooding” in our study). These parameters are defined for each wavelet packet and gathered in a “feature” vector. It is supposed that each fault is characterized by specific features values and that a feature can characterize a single fault class. In this work, we defined two feature vectors  $f_1$  and  $f_2$  for each packet:

$f_1$  is a vector gathering the normalized energy  $E^p$  (as expressed in Eq. (3) of all wavelet packets, and is defined by:

$$f_1 = [E^1; \dots; E^p; \dots; E^n]^t \quad (4)$$

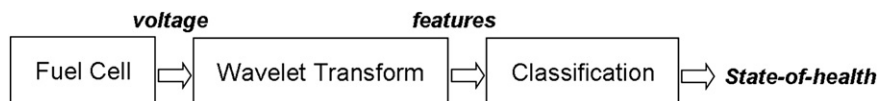


Fig. 1 – Principle of flooding diagnosis.

$-f_2$  is a vector gathering, for all wavelet packets, either the normalized energy  $E^p$  (as defined in Eq. (3)) divided by the energy of all the packets (if  $E^p$  is higher than a certain threshold value  $s_e$ ) or 0 (otherwise).  $s_e$  is a threshold value defined by trial-error approach.

$$f_2 = [f_2^1; f_2^2; \dots; f_2^p; \dots; f_2^n]^t, \quad \text{with} \quad \begin{cases} f_2^p = \frac{E^p}{\sum_{i=1}^n E^i} & \text{if } E^p > s_e \\ f_2^p = 0 & \text{otherwise} \end{cases} \quad (5)$$

where  $n$  is the total number of the wavelet packets.

### 3. Experimental application

#### 3.1. Fuel cell technical description

The data used in the simulation are collected from a 20-cells PEFC stack that has been assembled with a sprayed catalyst layer (Gore MESGA Primea Series 5510) and graphite distribution plates. Table 1 summarizes some characteristics of the investigated fuel cell stack.

#### 3.2. Test bench description

The experiments have been performed in a “in house” developed 1 kW test bench. Number of physical parameters involved in the stack can be controlled (gas flows, fluid hygrometry rates, air dew point temperature, stack temperature, load current)

**Table 1 – Technical specifications of the fuel cell used.**

Number of cells	20
Cell area (cm <sup>2</sup> )	100
Membrane thickness	25 μm
Platinum load (anode & cathode)	0.4 mg cm <sup>-2</sup>
Reactant stoichiometry ratio (anode/cathode)	Nominal = 2/4
Operating temperature (°C)	20–65
Operating pressure (bar)	Maximum 1.5 abs (0.5 relative)
Nominal output power (W)	500

and measured (inlet and outlet flows, pressures, temperatures, stack and single cell voltages). The control and the data acquisition process are based on National Instruments systems (PXI–SCXI set and Labview software). A simplified scheme for the test bench is proposed in Fig. 4.

The gas flow rates is fixed thanks to mass flow controllers. An automatic adjustment of the mass flows according to the load current level can be made (experiments have been achieved with constant anode/cathode stoichiometry factors).

The reactive gases can be humidified before their introduction to the FC stack: regulation of the air dew point temperature controls the air humidifying, which means that the air stream is forced through a bubbler (tank filled with deionised water) and maintained at the selected temperature level. The stack temperature is also controlled, namely through a demineralised water circuit. More details about the test bench used have been previously published in [20].

#### 3.3. Description of the test protocol

The flooding was emulated by increasing the inlet gases dew point temperature in order to favor water condensation: the dew point temperature is defined as the temperature below which, a part of water contained in the reactant gas condensate into liquid, i.e. at dew temperature, gas is saturated and its relative humidity equals 100%.

In total, 35 experiments were performed including 25 experiments in flooding conditions and 10 in “non flooding” conditions.

Fig. 5 shows the voltage and temperature evolutions recorded during one of the flooding experiments. The correlation between dew point increase and fuel cell voltage decrease indicates the presence of flooding, since the power decay is quite fast and no other parameter was changed. The low-amplitude oscillations ( $\pm 1$  °C) that one can observe on fuel cell stack temperature are directly linked to the temperature regulation on test bench.

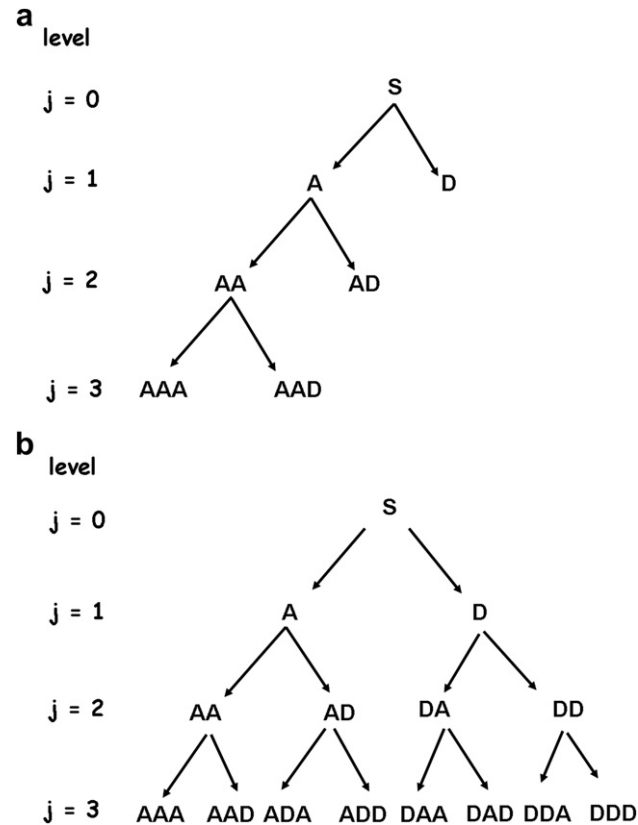


**Fig. 3 – (a) Wavelet decomposition at level 3, (b) Wavelet packets decomposition at level 3.**

## 4. Results and discussion

#### 4.1. Algorithm

A PEFC diagnosis algorithm, based on the Daubechies wavelet [18] to perform the wavelet analysis has been implemented on MATLAB using the “wavelet toolbox” [21]. In this analysis, all signals obtained during each experiments (flooding and non



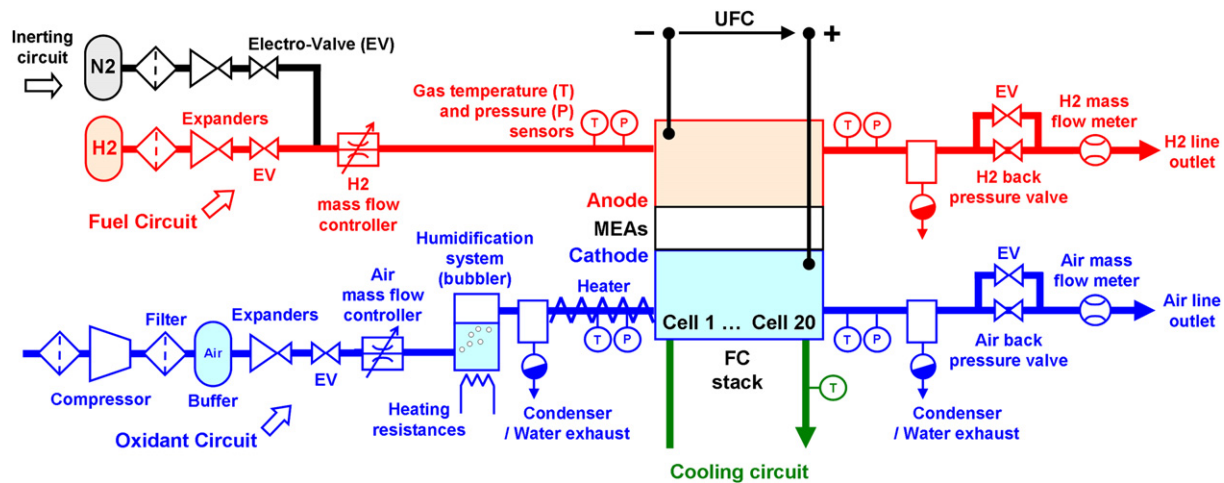


Fig. 4 – scheme of the test bench used [21].

flooding) were transformed into WP domain using Daubechies wavelets [18] at level 3. Consequently, as shown in Fig. 3b, we obtain 14 packets (the original signal is not considered). The sampling frequency for each signal is 6Hz and the threshold value is empirically set to  $s_e = 10^{-4}$ .

In order to classify the cell voltage behaviour, we determined, for each experiment, the two feature vectors  $f_1$  and  $f_2$  respectively defined by (Eq. (4)) and (Eq. (5)). For each of them, we define a “class matrix” that gathers the feature vectors determined for each experiment (in our case: 35). These matrix will therefore have the dimension  $n \times n_x$  where  $n$  is the number of wavelet packets and  $n_x$  is the total number of experiments corresponding to the class.

#### 4.2. Results

In order to allow the classification, features which dominate one signal class must be distinct from features which dominate another signal class. A preliminary analysis of data used in each class is thus performed in order to check whether the

data collected within the same class exhibit a similar behaviour. To reach this aim, the singular values  $\sigma_{i,x}^{v=1,2}$  and vectors of each class matrix are calculated according to the Singular Value Decomposition (SVD) method [22].

For a given matrix, an “effective rank”  $d_x$  is defined according the equation (Eq. (6)). It measures the effective dimensionality and corresponds to the number of significant singular values.

$$d_x = \frac{\sigma_{1,x} - \sigma_{2,x}}{\sigma_{1,x}} \quad (6)$$

Where  $\sigma_{1,x}$  and  $\sigma_{2,x}$  are the first and the second highest singular values coming from the SVD of the corresponding matrix.

As shown in Table 2 in the case of energy matrix, the  $d_x$  value determined for both classes (“flooding” and “no flooding”) and feature  $f_1$  is close to 1. This indicates that each matrix describes specifically a class. The same analysis was made for feature  $f_2$ , confirming the results, thus demonstrating that each fault is characterized by specific features values and that a feature can characterize a single fault class.

A statistical data representation of energy feature  $f_1$ , computed using Eq. (4) for the 14 packets and for each class, is given in Fig. 6. It shows that this feature exhibits different behaviour for each packet.

Fig. 6 shows that the packets 1, 3 and 7 are appropriate to discrimination. We choose the packet number 7 since the corresponding energy value is the highest one and we represented, in Fig. 7, the 2 features  $f_1$  and  $f_2$  obtained for this packet number ( $f_1^7$ ,  $f_2^7$ ) on the same plane. This graph shows that the features over this packet offer good separation ability between both states.

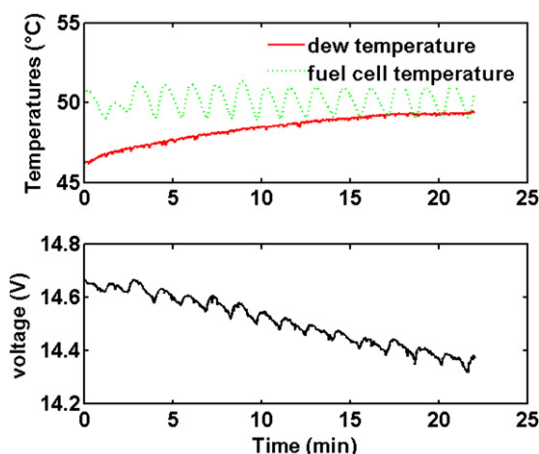


Fig. 5 – Experimental flooding induced during testing.

Table 2 – Singular values and effective rank of energy matrix of both classes.

Class	$\sigma_{1,x}$	$\sigma_{2,x}$	$d_x$
Flooding	38.6089	1.8740	0.9515
No flooding	22.0071	2.0989	0.9046

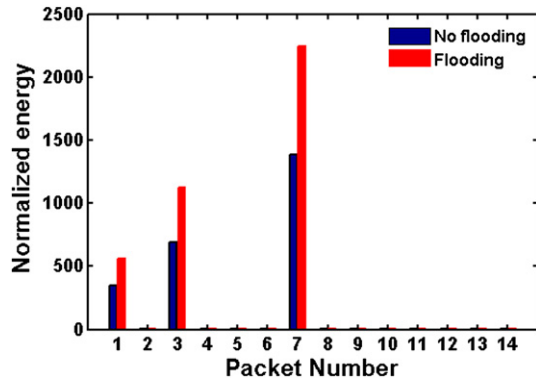


Fig. 6 – Statistical representation of the features contained for “flooding” and “non flooding” signals (energy contained in each packet).

Therefore, the features have only been restricted to packet 7, in order to reduce the size of discrimination data from  $(14 \times 35)$  times  $f_{i,i}$  ( $i=1,2$ ) to only a vector  $(1 \times 35)$  times  $f_{i,i}^T$  ( $i=1,2$ ).

Fig. 7 represents the results of the projection of the features corresponding to the flooding experiments (red crosses) and no flooding (blue rounds) ones. The projected features occupy two different area of the plane, which could be separated by a simple linear function.

Thus, the two features  $f_1$  and  $f_2$  at node 7 define a two dimensional plane who the states are easily separated.

#### 4.3. Discussion

The work presented aims at demonstrating the feasibility of the diagnosis by wavelets in PEFC domain. The algorithm used belongs to Pattern Recognition class of diagnosis approaches. It is based entirely on the experimental results, without any need to model the system structure: this point is one of the strengths of this diagnosis approach. However, despite the good separation ability of the two fuel cell's state of health shown by Fig. 6, this initiatory work has to be continued and improved.

The first improvement is to adapt the algorithm to an online, real time diagnosis; according to the simple scheme

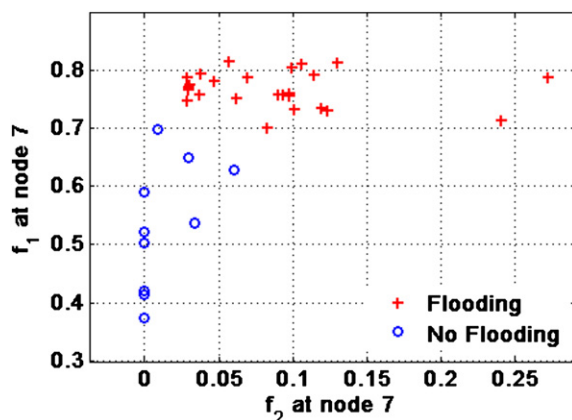


Fig. 7 – Features cluster using the two features  $f_1^T$  and  $f_2^T$ .

presented by [23]. Their adaptation of the Mallat algorithm permits computing the wavelet coefficients continuously, as soon as adequate data is available. On the other hand, features reduction and selection as well as the discrimination must be automated: using statistical criterions methods is widely used and gives good results. Finally, the present method gives a global state of health of the fuel cell and do not localize the flooding. In order to have such localisation, the diagnosis has to be applied on each individual cell using single cells voltage instead of stack voltage. The points raised above as well as the consideration of other faults in PEFC are currently in development in our laboratory.

## 5. Conclusion

In this study, the state of health of a fuel cell has been diagnosed only from the analysis of its voltage signal, which is the easiest and costless variable to monitor in a fuel cell system. The feasibility and the reliability of using such method to classify correctly PEFC states into flooded and non-flooded cell have been proven in this paper. It is therefore a very promising method and its application to other faulty operation states is currently under development in our laboratory.

Overcoming the major fuel cell difficulty which is identifying the inner parameters either for transportation or cogeneration application increases its relevance in the frame of diagnosis/supervision and also reliability purposes. This work takes into account only two fuel cell states; it could however be easily extended to other kind of faulty operation states as soon as the analyzed signal is directly affected with the fault. Such extension will be among the next improvements of this diagnosis tool. In near future, we will also focus on improvements of the automation of features reduction and classification, which could be achieved through the use of statistical methods.

## Acknowledgment

The authors would like to thank the French National Research Agency (ANR), in the scope of its national action plan for hydrogen (PAN-H) for financially supporting this work.

## REFERENCES

- [1] St Pierre J, Wilkinson DP, Knights S, Bos ML. Relationships between water management, contamination and lifetime degradation in PEFC. *Journal of New Materials for Electrochemical Systems* 2000;3:99–106.
- [2] Yousfi-Steiner N, Moçotéguy P, Candusso D, Hissel D, Hernandez A, Aslanides A. A review on PEM voltage degradation associated with water management: Impacts, influent factors and characterization. *Journal of Power Sources* 2008;183:260–74.
- [3] Wilkinson DP, St-Pierre J. Durability. In: Vielstich W, Lamm A, Gasteiger H, editors. *Handbook of fuel cells: fundamentals technology and applications*. England: Wiley; 2003. p. 611–26.

- [4] Yousfi Steiner N, Moçotéguy P, Candusso D, Hissel D. A review on PEM fuel cell catalyst degradation and starvation issues: causes, consequences and diagnostic for mitigation. *Journal of Power Sources* 2009;194:130–45.
- [5] Collier A, Wang H, Zi Yuan X, Zhang J, Wilkinson DP. Degradation of polymer electrolyte membranes. *International Journal of Hydrogen Energy* 2006;31:1838–54.
- [6] Hinaje M, Sadli I, Martin JP, Thounthong P, Raël S, Davat B. Online humidification diagnosis of a PEMFC using a static DC-DC converter. *International Journal of Hydrogen Energy* 2009;34:2718–23.
- [7] Springer TE, Rockward T, Zawodzinski TA, Gottesfeld S. Model for polymer electrolyte fuel cell operation on reformat feed effects of CO, H<sub>2</sub> dilution, and high fuel utilization. *Journal of the Electrochemical Society* 2001;148: A11–23.
- [8] Tian G, Wasterlain S, Endichi I, Candusso D, Harel F, Francois X, et al. Diagnosis methods dedicated to the localisation of failed cells within PEMFC stacks. *Journal of Power Sources* 2008;182:449–61.
- [9] Hissel D, Pera MC, Kauffmann JM. Diagnosis of automotive fuel cell power generators. *Journal of Power Sources* 2004; 128:239–46.
- [10] Chen J, Zhou B. Diagnosis of PEM fuel cell stack dynamic behaviors. *Journal of Power Sources* 2008;177:83–95.
- [11] Peng ZK, Chu FL. Application of the wavelet transform in machine condition monitoring and fault diagnostics: a review with bibliography. *Mechanical Systems and Signal Processing* 2004;18:199–221.
- [12] Zhu K, Wong YS, Hong GS. Wavelet analysis of sensor signals for tool condition monitoring: a review and some new results. *International Journal of Machine Tools and Manufacture* 2009;49:537–53.
- [13] Choi S. Detection of valvular heart disorders using wavelet packet decomposition and support vector machine. *Expert Systems with Applications* 2008;35:1679–87.
- [14] Ting W, Guo-zheng Y, Bang-hua Y, Hong S. EEG feature extraction based on wavelet packet decomposition for brain computer interface. *Measurement* 2008;41:618–25.
- [15] Behroozmand R, Almasganj F. Optimal selection of wavelet-packet-based features using genetic algorithm in pathological assessment of patients' speech signal with unilateral vocal fold paralysis. *Computers in Biology and Medicine* 2007;37:474–85.
- [16] Yin Y, Yu H, Zhang H. A feature extraction method based on wavelet packet analysis for discrimination of Chinese vinegars using a gas sensors array. *Sensors and Actuators B: Chemical* 2008;134:1005–9.
- [17] Mallat S. *A wavelet tour of signal processing*. Elsevier; 1999.
- [18] Daubechies. *Ten lectures on wavelets*. SIAM; 1992.
- [19] Misiti M, Misiti Y, Oppenheim G, Poggi J-M. *Les ondelettes et leurs applications*. Paris: Lavoisier; 2003.
- [20] D. Candusso, A. De Bernardinis, M.-C. Pera, F. Harel, X. Francois, D. Hissel, et al. Fuel cell operation under degraded working modes and study of diode by-pass circuit dedicated to multi-stack association, *Energy Conversion and Management*, in press, Corrected Proof.
- [21] Mathworks, [www.mathworks.com](http://www.mathworks.com), accessed 01.01.10
- [22] Golub GH, Kahan W. Calculating the singular values and pseudo-inverse of a matrix. *Journal of the Society for Industrial and Applied Mathematics: Series B, Numerical Analysis* 1965;2:205–24.
- [23] Bakshi BR, Stephanopoulos G. Compression of chemical process data by functional approximation and feature extraction. *American Institute of Chemical Engineers* 1996; 42:477–92.